



Contents lists available at ScienceDirect

## Journal of Controlled Release

journal homepage: [www.elsevier.com/locate/jconrel](http://www.elsevier.com/locate/jconrel)

## Targeting of tumor endothelium by RGD-grafted PLGA-nanoparticles loaded with Paclitaxel

Fabienne Danhier<sup>a</sup>, Benoît Vroman<sup>a</sup>, Nathalie Lecouturier<sup>a</sup>, Nathalie Crockart<sup>a</sup>, Vincent Pourcelle<sup>b</sup>, H  l  ne Freichels<sup>c</sup>, Christine J  r  me<sup>c</sup>, Jacqueline Marchand-Brynaert<sup>b</sup>, Olivier Feron<sup>d</sup>, V  ronique Pr  at<sup>a,\*</sup>

<sup>a</sup> Universit   Catholique de Louvain, Unit   de Pharmacie Gal  nique, Avenue Mounier, 73-20, 1200 Brussels, Belgium

<sup>b</sup> Universit   Catholique de Louvain, Unit   de Chimie Organique et M  dicinale, Place Louis Pasteur, 1, 1348 Louvain-la-Neuve, Belgium

<sup>c</sup> Universit   de Li  ge, Centre d'Etude et de Recherche sur les Macromol  cules, Sart Tilman B6, 4000 Li  ge, Belgium

<sup>d</sup> Universit   Catholique de Louvain, Laboratoire de Pharmacologie et de Th  rapeutique, Avenue Mounier 53-49, 1200 Brussels, Belgium

### ARTICLE INFO

#### Article history:

Received 11 May 2009

Accepted 5 August 2009

Available online 20 August 2009

#### Keywords:

Paclitaxel

RGD

Nanoparticles

PLGA

Tumor targeting

Tumor endothelium

### ABSTRACT

Paclitaxel (PTX)-loaded PEGylated PLGA-based nanoparticles (NP) have been previously described as more effective *in vitro* and *in vivo* than Taxol<sup>  </sup>. The aim of this study was to test the hypothesis that our PEGylated PLGA-based nanoparticles grafted with the RGD peptide or RGD-peptidomimetic (RGDp) would target the tumor endothelium and would further enhance the anti-tumor efficacy of PTX. The ligands were grafted on the PEG chain of PCL-b-PEG included in the nanoparticles. We observed *in vitro* that RGD-grafted nanoparticles were more associated to Human Umbilical Vein Endothelial cells (HUVEC) by binding to  $\alpha_v\beta_3$  integrin than non-targeted nanoparticles. Doxorubicin was also used to confirm the findings observed for PTX. *In vivo*, we demonstrated the targeting of RGD and RGDp-grafted nanoparticles to tumor vessels as well as the effective retardation of TLT tumor growth and prolonged survival times of mice treated by PTX-loaded RGD-nanoparticles when compared to non-targeted nanoparticles. Hence, the targeting of anti-cancer drug to tumor endothelium by RGD-labeled NP is a promising approach.

   2009 Elsevier B.V. All rights reserved.

### 1. Introduction

Although cancer cells are inherently more vulnerable to chemotherapy than the majority of normal cells, most anti-cancer drugs are non-selective and can cause injury to normal tissues. Efforts are now focused on attempts to kill cancer cells by more specific targeting while sparing normal cells [1–3]. Nanoparticles can target tumors by a passive or active process. Passive targeting implies that nanoparticles smaller than the fenestrations of endothelial cells can enter the interstitium and be entrapped in the tumor. The combination of leaky vasculature and poor lymphatic drainage results in the well-known Enhanced Permeability and Retention (EPR) effect [4]. Active targeting involves drug delivery to a specific site based on molecular recognition. One approach is to couple a ligand to nanoparticles which can interact with its receptor at the target cell site [5,6].

Angiogenesis, the development of new blood vessels, plays a critical role in controlling tumor growth and metastasis. Angiogenic endothelial cells may be considered as a major target for therapeutic intervention because they are easily accessible [7,8]. The interaction of integrin adhesion molecules  $\alpha_v\beta_3$  with specific ligands plays a key role in

angiogenesis [9]. The  $\alpha_v$  integrin (especially  $\alpha_v\beta_3$ ) are highly expressed on endothelial cells lining tumor and tumor cells but poorly expressed in resting endothelial cells and most normal organs, making it a potential target for anti-angiogenesis strategy [10]. Targeting the  $\alpha_v\beta_3$  integrin with drugs may provide an opportunity to target the tumor endothelium and to destroy tumor vessels without the harmful effects on the microvessels of normal tissue [10,11]. The tripeptide arginine–glycine–aspartic acid (RGD) has been shown to bind preferentially to particular integrin  $\alpha_v\beta_3$  [12,13]. Several non-peptide mimics of this tripeptide (named RGD-peptidomimetics), endowed with similar activity, have been developed for therapeutical uses [14,15], as well as for applications in biomaterials sciences [16,17], due to their stability in biological fluids.

Paclitaxel (PTX), a major anti-cancer drug isolated from the bark of *Taxus brevifolia*, has anti-neoplastic activity particularly against various types of solid tumors. PTX is approved in many countries for use as a second line treatment of ovarian and breast cancers [18]. Taxanes, like PTX, have a unique mechanism of action. PTX disrupts the dynamic equilibrium within the microtubule system and blocks cells in the late G<sub>2</sub> phase and M phase of the cell cycle, thereby inhibiting cell replication [19]. PTX is poorly soluble in water. To enhance its solubility and allow parenteral administration, PTX is currently formulated at 6 mg/ml in a vehicle composed of a 1:1 blend of Cremophor<sup>  </sup> EL and ethanol (Taxol<sup>  </sup>). However, Cremophor<sup>  </sup> EL causes side effects e.g. hypersensitivity, nephrotoxicity and neurotoxicity and alters endothelial function

\* Corresponding author. Tel.: +32 2 7647320; fax: +32 2 7647398.

E-mail address: [veronique.preat@uclouvain.be](mailto:veronique.preat@uclouvain.be) (V. Pr  at).

causing vasodilatation, labored breathing, lethargy and hypotension [20].

Previously, we developed PTX-loaded PEGylated PLGA-based nanoparticles showing a better  $IC_{50}$  *in vitro* and improved *in vivo* anti-tumor efficacy when compared to Taxol® [21]. Poly(lactide-co-glycolide) (PLGA) was chosen for its biodegradability properties, its biocompatibility and its approval by the FDA. Poly( $\epsilon$ -caprolactone-*b*-ethylene glycol) (PCL-*b*-PEG), an amphiphilic copolymer, was added to take advantage of the repulsive properties of PEG, to provide a higher stability of nanoparticles in biological fluids and to allow the grafting of an RGD peptide or RGD-peptidomimetic [22–24].

In this study, we checked the hypothesis that these PEGylated PLGA-based nanoparticles grafted with the RGD peptide or RGD-peptidomimetic would target the tumor endothelium and would further enhance the anti-tumor efficacy of PTX as compared to non-targeted PTX-loaded nanoparticles [21].

## 2. Material and methods

### 2.1. Nanoparticles formulation

#### 2.1.1. Polymer synthesis and characterization

PLGA was prepared as previously described by copolymerization of lactide and glycolide promoted by the dibutyltin dimethoxide (Sigma-Aldrich, St Louis, MO, USA) as the catalyst. To obtain the fluorescent polymer, fluorescein with a carboxylic acid function was prepared according to the method described previously [25] and then was coupled to the MeO-PLGA-OH using *N,N'*-dicyclohexylcarbodiimide as the coupling agent and 4-(dimethylamino)pyridine as the catalyst. PEG-*b*-PLGA was synthesized as previously described [26] by a conventional ring-opening polymerization of *D,L*-lactide and glycolide using PEG as the macroinitiator and stannous octanoate as the catalyst. The PEG-*b*-PCL copolymer was also synthesized by ring-opening polymerization using triethylaluminum as the catalyst [27]. The structure of the RGD peptide (A) and RGD-peptidomimetic (B) used in this study is shown in Fig. 1. The RGD-peptidomimetic (based on the tyrosine template) was prepared from (1)-tyrosine as scaffold, according to standard chemistry adapted from Kessler et al. [28] for the selective  $NH_2$  and OH functionalizations. The triethyleneglycol spacer-arm (for grafting on materials) was introduced via a sequence of reactions (nitration/reduction/acylation) adapted from Biltresse et al. [29,30].

#### 2.1.2. Photografting of PCL-*b*-PEG with RGD or RGD-peptidomimetic

PCL-*b*-PEG was solubilized in methylene dichloride or acetonitrile with *O*-succinimidyl 4-(*p*-azidophenyl) butanoate. After solvent evap-

oration, the polymer was dried under vacuum to constant weight and was removed from the plates as shaving. The polymer sample was irradiated at 254 nm in a quartz flask under an argon atmosphere for 20 min. After washing, the “activated” polymer was immersed in a 1 mM solution of ligand (GRGDS (NeoMPS, Strasbourg, France) or RGD-peptidomimetics in phosphate buffer (0.1 M): acetonitrile (1:1, v/v) at pH 8 and shaken for 24 h at 20 °C. The sample was then washed and dried under vacuum at 40 °C to a constant weight. [23,27].

#### 2.1.3. Preparation of Paclitaxel-loaded nanoparticles

Nanoparticles were prepared by nanoprecipitation. Briefly, 10 ml of acetone containing PLGA or fluorescent-PLGA (70 mg), PLGA-*b*-PEG (15 mg), PCL-*b*-PEG or PCL-*b*-PEG-*g*-GRGDS or PCL-*b*-PEG-*g*-RGD-peptidomimetic (15 mg) and PTX (1 mg) (Calbiochem, Darmstadt, Germany) was added to 20 ml of water under magnetic stirring at room temperature overnight. To remove the non-encapsulated drug, the suspensions were filtered (1.2  $\mu$ m) and ultracentrifuged at 22,000 g for 1 h at 4 °C. The pellets were suspended in adequate volume of ultra-purified water [21]. FITC-covalently labeled PLGA was used to prepare fluorescent nanoparticles.

The following nanoparticles were formulated:

- Non-loaded nanoparticles (NP): PLGA or fluorescent-PLGA (70 mg), PLGA-*b*-PEG (15 mg), PCL-*b*-PEG (15 mg)
- Non-loaded nanoparticles grafted with the RGD peptide (RGD-NP): PLGA or fluorescent-PLGA (70 mg), PLGA-*b*-PEG (15 mg), PCL-*b*-PEG-*g*-GRGDS (15 mg)
- Non-loaded nanoparticles grafted with the RGD-peptidomimetic (RGDp-NP): PLGA or fluorescent-PLGA (70 mg), PLGA-*b*-PEG (15 mg), PCL-*b*-PEG-RGD-peptidomimetic (15 mg)
- PTX-loaded nanoparticles (PTX-NP): PLGA or fluorescent-PLGA (70 mg), PLGA-*b*-PEG (15 mg), PCL-*b*-PEG (15 mg) and PTX (1 mg)
- PTX-loaded nanoparticles grafted with the RGD peptide (PTX-RGD-NP): PLGA or fluorescent-PLGA (70 mg), PLGA-*b*-PEG (15 mg), PCL-*b*-PEG-*g*-GRGDS (15 mg) and PTX (1 mg)
- PTX-loaded nanoparticles grafted with the RGD-peptidomimetic (PTX-RGDp-NP): PLGA or fluorescent-PLGA (70 mg), PLGA-*b*-PEG (15 mg), PCL-*b*-PEG-RGD-peptidomimetic (15 mg) and PTX (1 mg)

#### 2.1.4. Physicochemical characterization of Paclitaxel-loaded nanoparticles

The average size and size polydispersity of the nanoparticles were determined by photon correlation spectroscopy in water using a Malvern Nano ZS (Malvern Instruments, UK). The Zeta ( $\zeta$ ) potential of the nanoparticles was measured in KCl 1 mM with a Malvern Nano ZS at 25 °C. The instrument was calibrated with standard latex nanoparticles (Malvern Instruments, UK).

The drug loading efficiency was determined in triplicate by HPLC with UV detection at 227 nm (Agilent 1100 series, Agilent Technologies, Diegem, BE), as previously described [21]. The mobile phase (1.0 ml/min) consisted of acetonitrile and water (70:30 v/v, respectively). The reverse phase column was a CC 125/4 Nucleod UR 100-5 C18. The HPLC was calibrated with standard solutions of 5 to 100  $\mu$ g/ml of PTX dissolved in acetonitrile (correlation coefficient of  $R^2 = 0.99$ , LOD = 1.6  $\mu$ g/ml, LOQ = 5  $\mu$ g/ml, coefficients of variation <4.5%). Nanoparticles were dissolved in acetonitrile. The encapsulation efficiency was defined by the ratio of the measured amount of PTX encapsulated in nanoparticles to the initial amount of PTX encapsulated in nanoparticles, respectively. Experimental values were the average of at least 3 different formulations.

## 2.2. Association of nanoparticles to HUVEC

#### 2.2.1. Fluorescent and confocal microscopy

Human umbilical vein endothelial cells (HUVEC) (Clonetics, Lonza, Verviers, Belgium) were cultured in EGM-2 medium containing growth factors (Clonetics, Lonza, Verviers, Belgium) and serum at 37 °C in a 5%

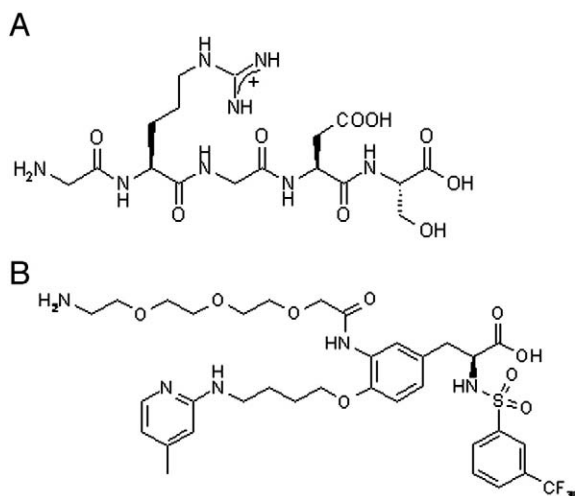


Fig. 1. Chemical structure of the RGD peptide (A) and the RGD-peptidomimetic (B).

CO<sub>2</sub>/95% air humidified atmosphere. To visualize the association of the nanoparticles with HUVEC,  $3 \times 10^5$  cells (passage 3) were plated in Lab-Tek 2-grid chamber pre-coated with 0.2% gelatin for 2 h. 2 days after plating, HUVEC were incubated for 2 h with fluorescent (FITC) nanoparticles containing PTX (PTX-NP and PTX-RGD-NP) (PTX concentration 25 µg/ml, polymer concentration approximately 3.66 mg/ml). After incubation, cells were washed 3X with HBSS (Gibco® BRL, Carlsbad, CA, USA), fixed with 4% paraformaldehyde in PBS and mounted with Vectashield (Vector Lab Inc., Burlingame, CA) containing DAPI. Cells were then examined using a fluorescent microscope (Axioskop 40, Zeiss) using the 350 nm (blue) and 470–490 nm (green) excitation filters and were photographed with an AxioCam MRC5 camera (Zeiss). The cells were also analyzed using a confocal laser scanning microscope (Axiovert 135 M microscope equipped with a Bio-Rad MRC1024 confocal system). Sequential images were processed and overlaid using Adobe Photoshop version 5.5.

*In vitro* competition assay was performed, using the same protocol that described above with some modifications. HUVEC (passage 3) were seeded in Lab-Tek 2-grid chamber and blocked with 5% BSA. A 20-fold molar excess of GRGDS peptide or the anti  $\alpha_v\beta_3$  integrin monoclonal antibody (1/50 dilution) (GeneTex, Irvine, USA) was pre-incubated for 15 min in serum-free medium [12]. Fluorescent RGD-NP were added to the HUVEC for 1 h at 37 °C.

To visualize the cellular distribution of both polymers and drugs, Doxorubicin (DOX) (Sigma-Aldrich, St Louis, MO, USA) was encapsulated in the same nanoparticles. Briefly, nanoparticles were prepared by nanoprecipitation as described previously, replacing PTX by 5 mg of DOX. The average size, size polydispersity and the Zeta ( $\zeta$ ) potential of the nanoparticles were measured. The drug content was determined after nanoparticles were dissolved in acetonitrile, using spectrophotometer (HP8453 from Hewlett Packard) at 481 nm. The association of DOX-loaded nanoparticles with HUVEC,  $3 \times 10^5$  cells (passage 4) was assessed in Lab-Tek 2-grid chamber as described above ( $n=4$ ). DOX-loaded nanoparticles or free nanoparticles were incubated 1 h at a concentration of 6 µg/ml DOX. Cells were then examined using a fluorescent microscope (Axioskop 40, Zeiss) using the 480 nm (red) excitation filters and were photographed with an AxioCam MRC5 camera (Zeiss) [31].

### 2.2.2. *In vitro* uptake

The amount of nanoparticles associated to endothelial cells was also quantified. Flat-bottom 48-well culture plates were coated with 0.2% gelatin for 2 h at room temperature and then blocked with 0.1% BSA for 30 min at 37 °C. HUVEC (passage 4) were resuspended in EGM-2 medium and plated at  $2 \times 10^4$  cells/well for 24 h. HUVEC were then activated with TNF- $\alpha$  (4 ng/ml) for 4 h to enhance  $\alpha_v\beta_3$  integrin expression [32,33]. Cells were then incubated with 200 µl of fluorescent (FITC) NP and RGD-NP (polymers concentration approximately 10 mg/ml) at 4 °C for 30 min and at 37 °C for 30 min, 1, 2 or 4 h. At designated times, cells were lysed with Triton X-100 (0.05% v/v) after rinsing with PBS to remove unattached cells. The amount of uptaken nanoparticles was quantified directly through measurement of fluorescence emission using a Packard Fluorocount Microplate fluorometer (Packard Instrument Company, Meriden, CT, USA). The fluorometer was calibrated with standard solution of 17.5 to 7000 µg/ml of fluorescent-PLGA (correlation coefficient of  $R^2=0.9985$ ). The excitation/emission wavelengths for FITC were 485/530 nm. Cellular uptake (%) was calculated from the ratio of FITC concentrations and the initial FITC concentration. The measured FITC concentrations were calculated from the measured fluorescence intensity and the calibration curve. [34].

A competition assay was performed by pre-incubating the activated cells with either a 20-fold molar excess of GRGDS peptide or with the anti  $\alpha_v\beta_3$  integrin monoclonal antibody (1/50 dilution) for 15 min in serum-free medium. Fluorescent NP were incubated for 4 h [12].

### 2.3. *In vivo* targeting of RGD-NP to tumor vasculature

#### 2.3.1. Tumor model

Syngeneic transplantable liver tumors (TLT) [21,35] were implanted in the gastrocnemius muscle in the rear leg of 8 week old male NMRI mice (Janvier, Genest St Isle, France). All experiments were performed in compliance with guidelines set by national regulations and were approved by the Ethical Committee For Animal Care of The Faculty of Medicine of the Université Catholique de Louvain. The treatments were applied when the tumor reached  $8.0 \pm 0.5$  mm (approximately 7 days). Before injection, animals were anesthetized by inhalation of Isoflurane mixed with 21% oxygen in a continuous flow (1.5 l/min) delivered by a nose cone.

#### 2.3.2. Immunohistochemistry

The fluorescent nanoparticles (NP, RGD-NP and RGDp-NP, 10 mg/ml; 100 µl) were injected through the tail vein of mice ( $n=4$ ). Two hours after injection, animals were sacrificed. Tumors were removed, covered with cryo-embedding compound OCT (Tissue-Tek, Sacura), snap frozen in liquid nitrogen and stored at  $-80$  °C until sectioning.

5 µm-sections were mounted onto charged superfrost-plus glass slides and stored at  $-80$  °C until staining. The sections were fixed in ice-cold acetone, rehydrated in PBS and immunostained with a rat anti-CD31 antibody (1:50) in 1% bovine serum albumin (BSA) in PBS for 1 h. This was followed by three rinses in PBS. Incubation with the secondary antibody Alexa 568 goat anti-rat (1:500) was conducted for 30 min at room temperature, followed by three washes in PBS. The sections were then mounted with Vectashield containing DAPI. Sections were analyzed using a fluorescent microscope with 350 nm (blue), 470–490 nm (green) and 515–560 nm (red) excitation filters [36]. Sequential images were processed and overlaid using Adobe Photoshop version 5.5.

#### 2.3.3. *In vivo* anti-tumor efficacy

When tumors reached  $8.0 \pm 0.5$  mm in diameter, the mice were randomly assigned to one of the following groups: group 1: PBS injection; group 2: non-loaded NP; group 3: PTX-NP; group 4: PTX-RGD-NP; group 5: PTX-RGDp-NP. All the treatments were injected through the tail vein (1 mg/kg PTX, approximately 138 mg/kg polymers in 100 µl of PBS). After treatment, tumors were measured every day with an electronic caliper until they reached a diameter of 18 mm, at which time the mice were sacrificed. Changes in body weight were also monitored.

### 2.4. Statistics

All results are expressed as mean  $\pm$  standard deviation. One-way or two-way ANOVA, Bonferroni post test and the Kaplan–Meier survival rate were performed using the software GraphPad Prism 5 for Windows (v 5.00, La Jolla, CA, USA) to demonstrate statistical differences ( $p < 0.05$ ). To allow statistical analysis, Adobe Photoshop version 5.5. was used to quantify the fluorescence from the microscopy images of Figs. 3 and 5.

**Table 1**  
Chemical description of the polymers included in the formulations.

Polymer	Mn (SEC) g/mol <sup>a</sup>	Mn (NMR) g/mol Polyester-PEG	Mol % glycolidel <sup>b</sup>
PLGA	22,000	–	25
Fluorescent-PLGA	23,600	–	29
PLGA-b-PEG	29,300	16,500–4,600	26
PCL-b-PEG	22,400	15,200–4,600	–

<sup>a</sup> Polystyrene calibration.

<sup>b</sup> Determined by NMR by the following formula:  $(I_{4.7}/2)/(I_{5.2} + I_{4.7}/2) \times 100$ , where  $I_{4.7}$  is the signal intensity of the glycolide unit at 4.7 ppm (CH<sub>2</sub>OC=O) and  $I_{5.2}$  is the signal intensity of the lactide unit at 5.2 ppm (CH(CH<sub>3</sub>)OC=O).

**Table 2**Physicochemical characteristics of the nanoparticles ( $n = 6$ ).

	PTX-NP	PTX-RGD-NP	PTX-RGDp-NP
PTX encapsulation efficiency (%)	72 ± 3	62 ± 2	64 ± 3
PTX/polymers (%)	0.72 ± 0.03	0.6 ± 0.02	0.7 ± 0.06
PTX recovery (%)	95.4 ± 1.2	96.2 ± 2.3	95.3 ± 4.2
Size (nm) <sup>a</sup>	114 ± 3	138 ± 3	146 ± 2
PDI <sup>a</sup>	0.11 ± 0.006	0.106 ± 0.004	0.12 ± 0.003
ζ potential (mV) <sup>b</sup>	−0.36 ± 4.3	−0.09 ± 2.6	0.12 ± 3.6
ζ deviation (mV) <sup>b</sup>	5.69 ± 1.03	5.47 ± 1.2	4.69 ± 1.6

<sup>a</sup> Measured by photon correlation spectroscopy with a Malvern Nano ZS.<sup>b</sup> Determined with a Malvern Nano ZS.

### 3. Results

#### 3.1. Physicochemical characterization of Paclitaxel-loaded nanoparticles

The composition and molecular weights of polymers synthesized by conventional ring-opening polymerization processes [37] and used in the formulations are summarized in Table 1. Nanoparticles were characterized in terms of size and ζ potential (Table 2). The size of PTX-NP was 114 nm, while the size of PTX-RGD-NP or PTX-RGDp-NP was slightly enhanced (138 and 146 nm, respectively). Nanoparticles exhibited a narrow size distribution (polydispersity index <0.2). ζ potential of nanoparticles was close to neutrality, confirming the presence of PEG chains shielding the negative charges present at the nanoparticle surface. Previously, we have shown that PEGylated

PLGA-based nanoparticles produced by nanoprecipitation presented 41% of PEG exposed at the nanoparticles surface [38]. The ligand grafting assessed by X-ray Photoelectron Spectroscopy (XPS), was approximately 0.4–0.5 molecules by PCL-b-PEG chain [23]. Consistent with previously published data [39], the presence of PTX compared to free-drug nanoparticles did not affect the size and the ζ potential of nanoparticles (data not shown).

The percentage of encapsulation of PTX-NP, PTX-RGD-NP and PTX-RGDp-NP was 72%, 61% and 64%, respectively.

#### 3.2. Association of NP and RGD-NP to HUVEC

##### 3.2.1. Fluorescent microscopy

To check if RGD-grafted nanoparticles could recognize  $\alpha_v\beta_3$  integrins on endothelial cells, the association of PTX-NP and PTX-RGD-NP to HUVEC that express the  $\alpha_v\beta_3$  integrins was assessed by fluorescent microscopy [40,41]. Compared to non-targeted PTX-NP, a high level of association of fluorescent PTX-RGD-NP with HUVEC was demonstrated (Fig. 2A and B). Confocal laser scanning microscopy (Fig. 2C) suggested both membrane and intracellular localization of PTX-RGD-NP.

To visualize the specificity of the RGD-NP for  $\alpha_v\beta_3$  integrin, we performed competition assay on HUVEC. Excess of GRGDS peptide (2) or anti  $\alpha_v\beta_3$  integrin monoclonal antibody (3) strongly inhibited the binding of the RGD-NP (1) to HUVEC (Fig. 2D).

To confirm these data on the localization of fluorescent NP formed with FITC-covalently bound to PLGA, we replaced PTX by fluorescent-DOX. The size and the ζ potential of DOX-loaded nanoparticles were 127 nm (PDI = 0.14 nm) and −0.23 mV, respectively. The percentage of

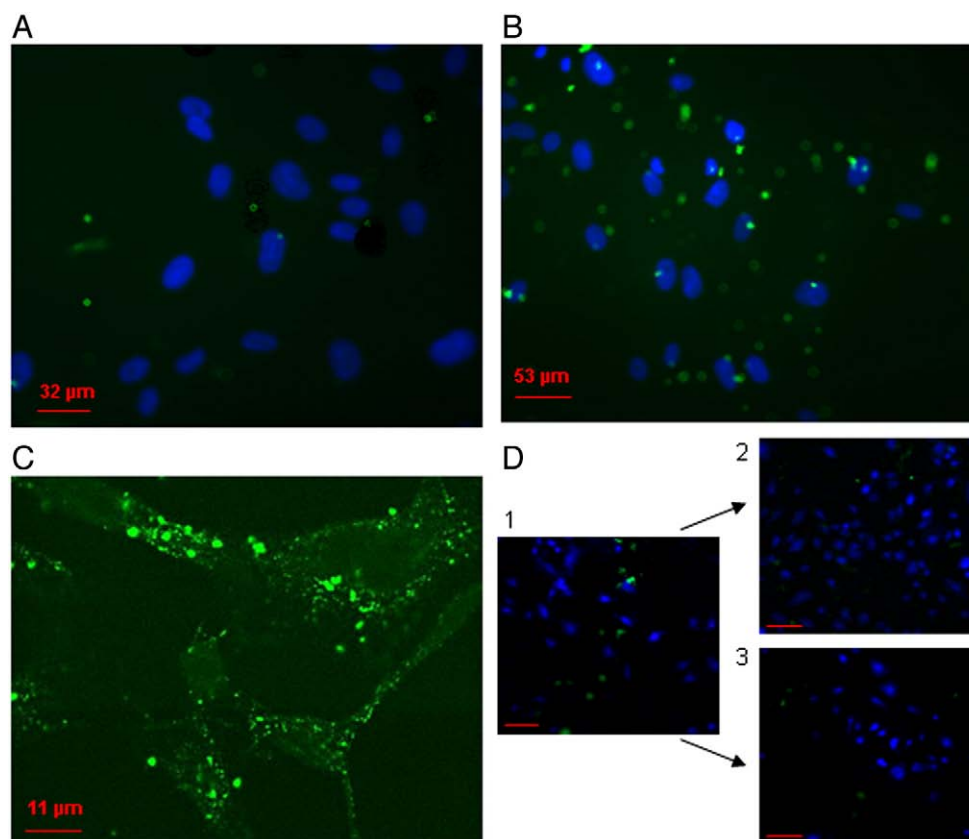


**Fig. 2.** Detection of fluorescent PTX-loaded nanoparticles in HUVEC. DAPI staining was used to label nuclei. Fluorescent microscopy of HUVEC incubated for 2 h with (A) PTX-NP and (B) PTX-RGD-NP. (C) Internalization of PTX-RGD-NP observed by confocal laser scanning microscopy. (D) Fluorescent microscopy of HUVEC incubated for 1 h with fluorescent RGD-NP. (1) No pre-treatment. (2) Pre-treatment with a 20-fold molar excess of the GRGDS peptide. (3) Pre-treatment with the anti  $\alpha_v\beta_3$  integrin monoclonal antibody (1/50 dilution). (Scale bars: D, 100 μm).

encapsulation was 88%. Compared to non-targeted DOX-NP or non-encapsulated DOX (free DOX), a high level of association of DOX from DOX-RGD-NP with HUVEC was demonstrated ( $p < 0.001$ ) (Fig. 3). The blue fluorescence (DAPI) was co-localized with DOX (red fluorescence) indicating that DOX accumulated in nuclei. Interestingly, non-targeted nanoparticles were more uptaken by HUVEC than free DOX ( $p < 0.01$ ), which is not in line with the most of publications. Nevertheless, Yoo et al. published similar results. This can be attributed to the fact that nanoparticles were more readily internalized by an endocytosis mechanism, while free DOX was transported into cells by a passive diffusion mechanism [42].

3.2.2. *In vitro* HUVEC uptake

To compare the association (binding and uptake) of NP, RGD-NP and RGDp-NP to HUVEC and to test for the selective binding of RGD(p)-NP to activated endothelial cells, we performed a quantitative endothelial cell uptake assay (Fig. 4A). TNF- $\alpha$  is known to promote  $\alpha_v\beta_3$  integrin expression at the surface of endothelial cells [32]. While activation of HUVEC by TNF- $\alpha$  did not influence the cellular uptake of non-targeted NP, the cellular uptake of RGD-NP and RGDp-NP was significantly enhanced by TNF- $\alpha$  incubation at all times tested ( $p < 0.001$ ). The uptake of RGDp-NP was enhanced as compared to non-targeted NP ( $p < 0.001$ ), indicating that the design of RGDp to bind to  $\alpha_v\beta_3$  integrin is a promising approach. However, the uptake of RGDp-NP was lower than RGD-NP ( $p < 0.001$ ).

When the GRGDS peptide or the anti  $\alpha_v\beta_3$  integrin monoclonal antibody was pre-incubated with TNF- $\alpha$  activated HUVEC, the cellular uptake of RGD-NP became equivalent to non-targeted NP, showing that the cellular uptake of RGD-NP was mediated by  $\alpha_v\beta_3$  integrin binding (Fig. 4B).

Other peptides, LDV peptide and LDV peptidomimetic (LDVp) were also grafted on the NP surface. LDV and LDVp were shown previously to

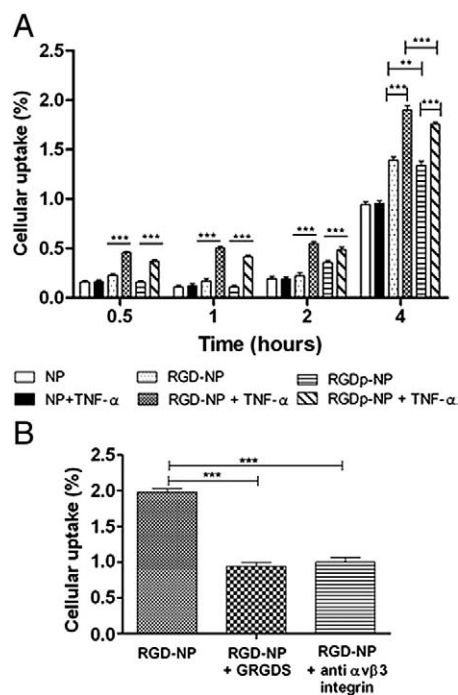


Fig. 4. (A) Uptake of fluorescent NP and RGD-NP by HUVEC incubated or not with TNF- $\alpha$  (4 ng/ml). (B) Competition assay for the *in vitro* uptake of RGD-NP by activated HUVEC. HUVEC were pre-treated for 15 min with a 20-fold molar excess of the GRGDS peptide or with the anti  $\alpha_v\beta_3$  integrin monoclonal antibody (1/50 dilution) ( $n = 6$ ). \*\*\* $p < 0.001$ .

enhance the transport of NP through  $\beta_1$  integrin binding [24]. *In vitro* HUVEC uptake showed no improvement as compared to non-targeted NP (data not shown).

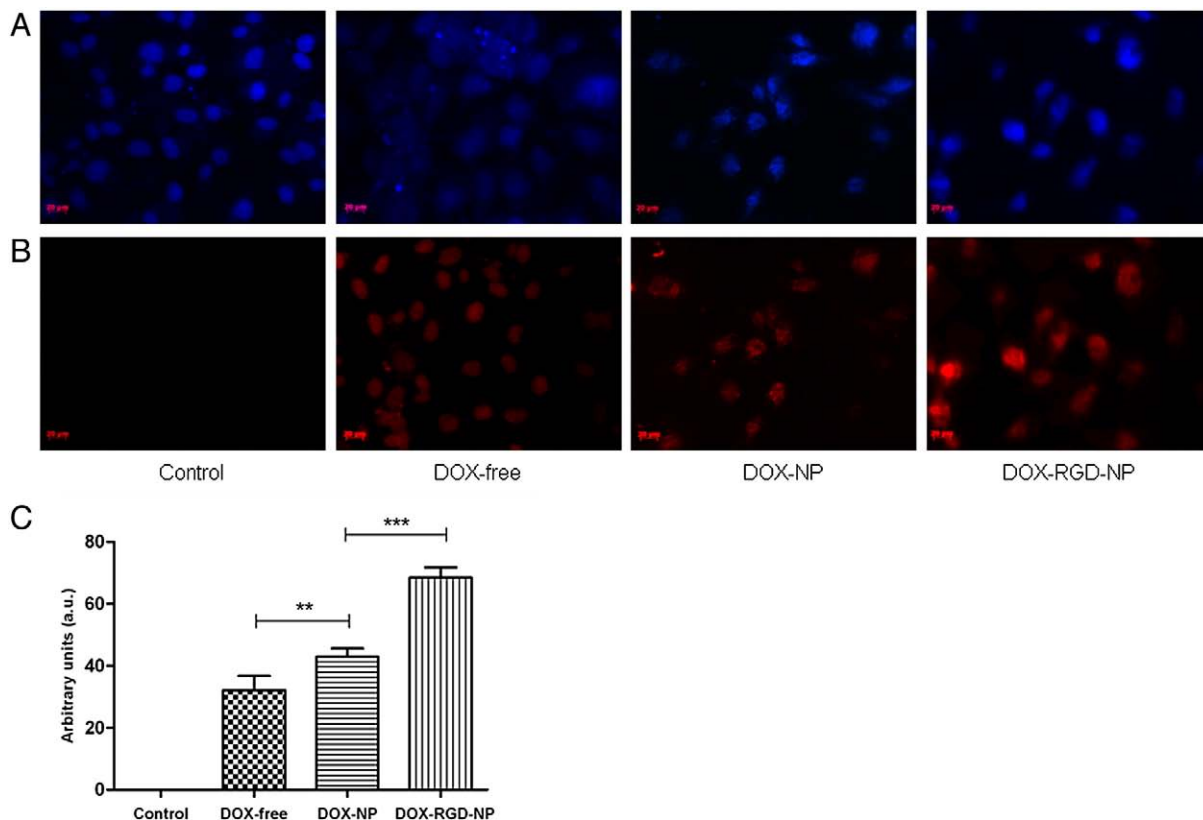


Fig. 3. Detection of DOX in HUVEC incubated for 1 h with free DOX, DOX-NP and DOX-RGD-NP (DOX concentration 6  $\mu\text{g/ml}$ ). DAPI staining was used to label nuclei. Fluorescent microscopy of (A) DAPI and (B) DOX. (C) Quantification of the fluorescent-DOX signal from HUVEC after incubation of free DOX, DOX-NP and DOX-RGD-NP ( $n = 4$ ). \*\*\* $p < 0.001$ .

### 3.3. *In vivo* targeting of the RGD-NP or RGDp-NP to tumor vasculature

To investigate whether RGD or RGDp-grafted nanoparticles could target tumor endothelium *in vivo*, fluorescent-PLGA-based NP, RGD-NP and RGDp-NP were injected intravenously in TLT (Transplantable Liver Tumor) tumor-bearing mice. Sequential sections of the tumor were analyzed for nuclear staining by DAPI (blue fluorescence), nanoparticles by modified fluorescein (green fluorescence), and blood vessels by CD31 immunohistochemistry (red fluorescence). As shown in Fig. 5, a higher green fluorescence was observed in the tumor upon RGD-NP injection when compared to non-targeted NP and RGDp-NP ( $p < 0.001$ ). Nevertheless, the green fluorescence associated to RGDp-NP was higher than non-targeted nanoparticles ( $p < 0.001$ ) indicating a better tumor targeting of nanoparticles grafted with the RGDp. The green fluorescence of nanoparticles was co-localized with CD31 immunostaining (red fluorescence) indicating that the nanoparticles targeted the tumor endothelium.

### 3.4. *In vivo* anti-tumor efficacy

The anti-tumor efficacy of non-loaded NP, PTX-NP, PTX-RGD-NP and PTX-RGDp-NP was evaluated in TLT tumor-bearing mice (PTX 1 mg/kg). PTX-RGD-NP inhibited tumor growth more efficiently than non-targeted PTX-NP and PTX-RGDp-NP. Tumor diameter reached 18 mm (endpoint of the experiment) on day 7 for control (PBS) group,

on day 12 for PTX-NP or PTX-RGDp-NP and on day 18 for PTX-RGD-NP ( $p < 0.001$ ) (Fig. 6A). The survival rate, determined from the time required by the tumors to reach 18 mm, was significantly higher for mice treated with PTX-RGD-NP as compared with non-targeted PTX-NP or PTX-RGDp-NP ( $p < 0.001$ ) (Fig. 6B). Non-loaded NP showed the same tumor growth curve than PBS, indicating that polymers were not cytotoxic ( $p > 0.05$ ). We have also shown previously that PTX-NP inhibited tumor growth more efficiently than Taxol® [21]. Body weight measurements showed no significant differences between the groups throughout the study. There was a slight increase in body mass as a result of natural animal growth (data not shown).

## 4. Discussion

Numerous investigations have shown that chemotherapeutic drugs can be delivered by their entrapment in submicronic colloidal systems. Non-targeted nanoparticles can passively accumulate in the tumor via the Enhanced Permeability and Retention (EPR) effect, improving their anti-tumor activity. Targeted delivery represents a potential approach to further enhance anti-tumoral efficacy and minimize toxicity [12]. Targeted delivery to tumor vasculature is considered a powerful strategy for cancer treatment since angiogenesis is essential for tumor growth.  $\alpha_v\beta_3$  integrins are minimally expressed on normal quiescent endothelial cells, but significantly upregulated on proliferating endothelium. Studies described that RGD-peptides have been introduced into proteins,

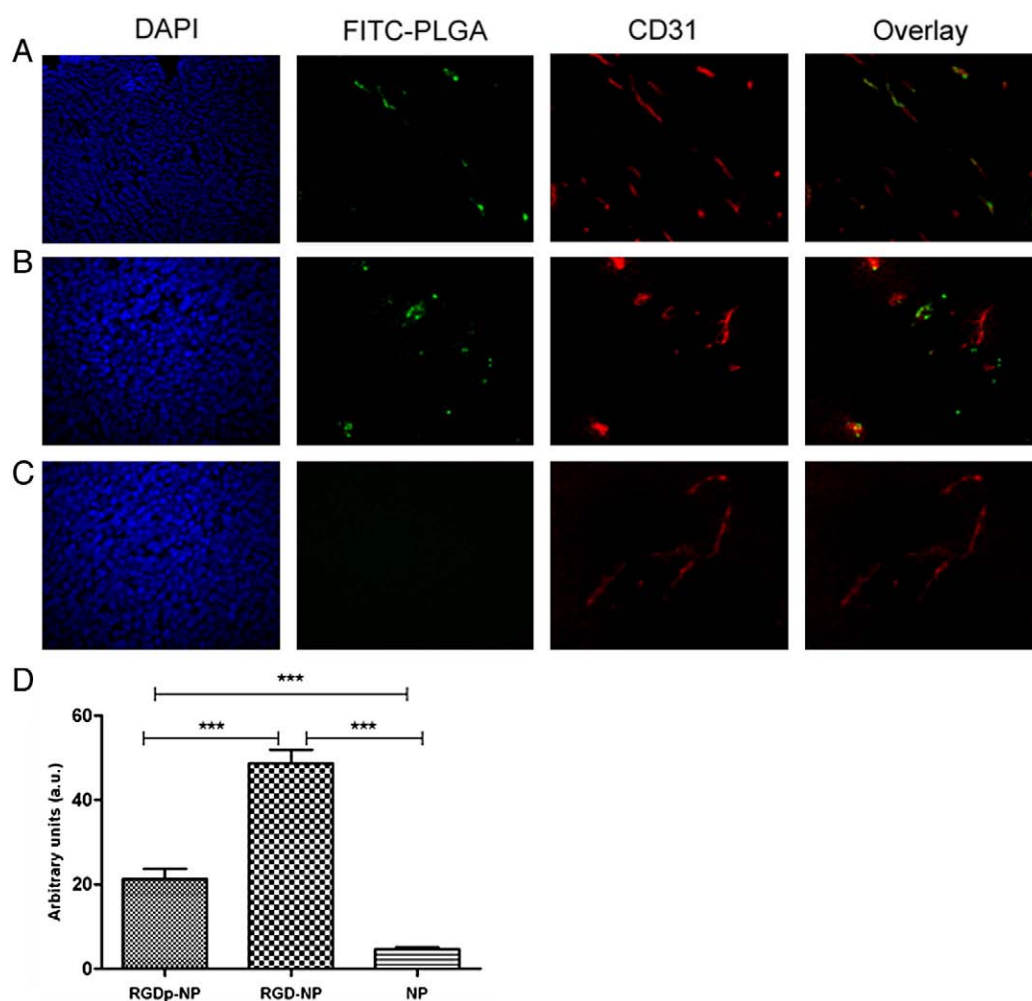


**Fig. 5.** Fluorescent microscopy of TLT tumors growing in NMRI mice 2 h after injection of NP containing fluorescent-PLGA (green). Sections were stained with anti-CD31 to label endothelial cells (red) and counterstained with DAPI for nucleus detection (blue). (A) RGDp-NP, (B) RGD-NP and (C) non-targeted NP. (D) Quantification of the fluorescent-PLGA signal from TLT tumors after NP, RGD-NP and RGDp-NP injection ( $n = 4$ ). \*\*\* $p < 0.001$ .

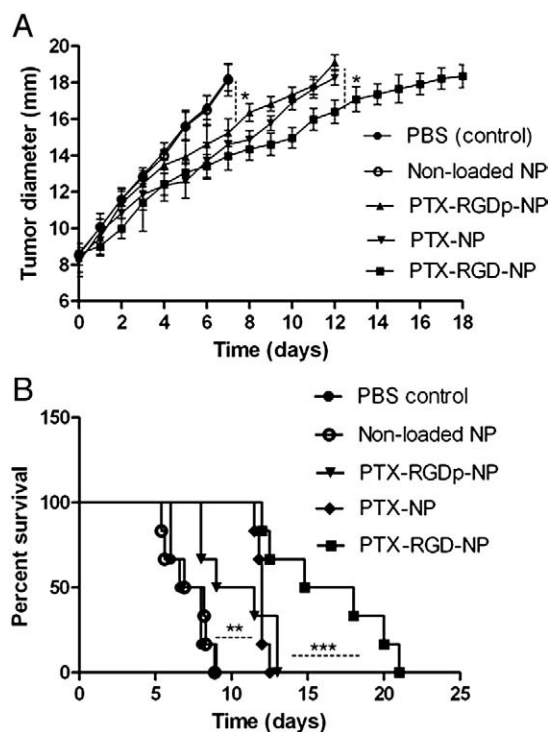


**Fig. 6.** Anti-tumor effect of non-loaded NP, PTX-NP, PTX-RGDp-NP and PTX-RGD-NP (PTX concentration: 1 mg/kg) on TLT tumor-bearing mice. (A) Tumor growth delays curves. Mean of tumor size  $\pm$  SEM ( $n=6$ ). (B) Survival rates of tumor-bearing mice. \*  $p < 0.05$ , \*\*  $p < 0.01$ , \*\*\*  $p < 0.001$ .

polymers, liposomes, micelles, viruses and gene delivery vehicles to improve diagnosis via imaging or to deliver therapeutics to solid tumors [15,17,31,40,43].

In this study, using both *in vitro* and *in vivo* evaluations, we demonstrated the ability of nanoparticles grafted with the RGD peptide to target the tumor endothelium (via the binding to  $\alpha_v\beta_3$  integrin) and improve the anti-tumoral efficacy of PTX. Fluorescent and confocal microscopy showed that PTX-RGD-NP were significantly more associated to HUVEC than PTX-NP due to their ability to bind preferentially the  $\alpha_v\beta_3$  integrin, as indicated by the inhibitory effect of anti  $\alpha_v\beta_3$  integrin (Fig. 2). Both membrane and intracellular localization of RGD-NP were observed. As reported previously [44,45], the binding of the RGD peptide to the  $\alpha_v\beta_3$  integrins expressed by the endothelial cells is very likely to account for the signal detected at the membrane level. The observed pattern of intracellular perinuclear localization of the nanoparticles suggests an endocytic uptake mechanism and lysosomal localization. The  $\alpha_v\beta_3$  integrins have been reported to pass rapidly through endosomes, ending to the perinuclear compartments approximately 30 min after internalization [46]. Generally, nanoparticles are non-specifically internalized into cells via endocytosis or phagocytosis [47,48]. These results suggest that RGD-NP could be internalized preferentially by endothelial cells lining tumor blood vessels.

Consistent with this hypothesis, an increased cellular uptake of RGD-NP but not non-targeted NP by activated HUVEC was observed (Figs. 2C and 4). The selective accumulation of leukocytes in the tumor is guided by endothelial adhesion molecules (EAM). Expression of EAM is controlled by cytokines such as tumor necrosis factor  $\alpha$  (TNF- $\alpha$ ). Activation of endothelial cells by TNF- $\alpha$  induces a measurable level of upregulation of EAM of endothelial cells [32,33]. Competition assay clearly demonstrated the specificity of the RGD-NP for  $\alpha_v\beta_3$  integrin expressed in the tumor endothelium (Figs. 2D and 4B).

*In vivo* immunohistochemistry on TLT-tumor-bearing mice demonstrated that RGD-NP targeted the tumor endothelium more precisely,

when compared to non-targeted NP. Administration of PTX-RGD-NP at a dose of 1 mg/kg resulted in effective delay of tumor growth and prolonged survival times when compared to PTX-NP. When encapsulated into non-targeted nanoparticles, PTX could reach the tumor site through the EPR effect and maintain the effective therapeutic concentration for a long period of time. These PTX-NP were more effective than Taxol<sup>®</sup> at delaying tumor growth [21]. Concerning PTX-RGD-NP, the combined effect of passive accumulation and specific tumor targeting contributed to significantly improve the therapeutic efficacy of PTX. These results show the major interest to nano-formulate poorly soluble chemotherapeutic drug, particularly with targeted nanoparticles. It is also interesting to note that non-loaded NP were not cytotoxic both *in vitro* [21] and *in vivo*.

The second aim of this paper was to check if RGDp could be used to increase the targeting of NP to tumor endothelium. The synthesis of non-peptide mimic of the RGD sequence is an approach which consists in increasing the affinity of the ligand to its receptor and to enhance the stability of the ligand by suppressing the peptide link which can be degraded by enzymes [30]. The *in vitro* data confirm that replacing RGD by RGDp allowed enhanced association and binding to HUVEC as compared to non-targeted NP. However, even though the peptidomimetics were designed to enhance the stability of RGD *in vivo*, no improvement of PTX efficacy was observed by encapsulation of PTX into RGDp-NP. RGDp has been recently shown to interact with the beta 1 and beta 3 sub-types [29,30], did not show better results than the original RGD sequence for the targeting of the  $\alpha_v\beta_3$  integrin. Similar differences between *in vitro* and *in vivo* studies have been described in another study [24]. After IV injection, RGDp can bind to many other receptors before its accumulation in the tumor. Peptidomimetics may be considered as a promising approach in regard to *in vitro* data, but the design of the RGDp still need to be optimized because of the poor results obtained *in vivo*. Other peptidomimetics have been synthesized and will be tested in the near future.

## 5. Conclusion

The aim of the study was to design polymeric nanoparticles loaded with the anti-cancer drug PTX and to specifically target the tumor endothelium. The RGD peptide or a novel RGDp were grafted on the PEG chain of PCL-b-PEG included in the nanoparticles. *In vitro* studies with HUVEC showed an enhanced cellular uptake of the targeted RGD-NP when compared to non-targeted NP, mediated by the binding to the  $\alpha_v\beta_3$  integrin. The targeting of the RGD-NP or RGDp-NP to the tumor endothelium was also demonstrated in TLT tumor-bearing mice. This targeting was associated with a higher survival rate for mice treated with PTX-RGD-NP when compared to non-grafted PTX-NP. Our proof of concept *in vitro* and *in vivo* shows that our RGD-NP could have great advantages increasing their anti-cancer efficacy by targeting the anti-cancer drug to the tumor vasculature as compared to non-targeted NP. Promising results obtained *in vitro* but non *in vivo* with RGDp reveal that non-peptide mimics represent an attractive approach which would be optimized and developed in the future.

## Acknowledgments

The authors wish to thank Johnson & Johnson, Pharmaceutical Research and Development, Division of Janssen Pharmaceutica, Belgium for providing Paclitaxel. This work was supported by the FRSM (Belgium) (to VP and CJ) and the Fonds J. Maisin (to OF). The authors also thank Fouzi Kostet from the FATH Unit and Bernard Ucar from the FARG Unit (Université Catholique de Louvain, Brussels, Belgium) for their technical support. J. Marchand, H. Freichels, C. Jérôme and V. Pr at are grateful to the "R gion Wallonne" in the framework of the project VACCINOR for indirect financial support of this research.

## References

- [1] B. Haley, E. Frenkel, Nanoparticles for drug delivery in cancer treatment, *Urol. Oncol.* 26 (2008) 57–64.
- [2] M. Davis, Z. Chen, D. Shin, Nanoparticle therapeutics: an emerging treatment modality for cancer, *Nat. Rev. Drug Discov.* 7 (2008) 771–782.
- [3] T. Lammers, W. Hennink, G. Storm, Tumour-Target. *Nanomed.* 99 (2008) 392–397.
- [4] H. Maeda, J. Wu, T. Sawa, Y. Matsumura, K. Hori, Tumor vascular permeability and the EPR effect in macromolecular therapeutics: a review, *J. Control. Release* 65 (2000) 271–284.
- [5] J.D. Byrne, T. Betancourt, L. Brannon-Peppas, Active targeting schemes for nanoparticle systems in cancer therapeutics, *Adv. Drug Deliv. Rev.* 60 (2008) 1615–1626.
- [6] T. Allen, Ligand-targeted therapeutics in anticancer therapy, *Nat. rev., Cancer* 2 (2002) 750–763.
- [7] P. Carmeliet, R.K. Jain, Angiogenesis in cancer and other diseases, *Nature* 407 (2000) 249–257.
- [8] E. Ruoslahti, Specialization of tumour vasculature, *Nat. Rev., Cancer* 2 (2002) 83–90.
- [9] R.O. Hynes, A reevaluation of integrins as regulators of angiogenesis, *Nat. Med.* 8 (2002) 918–921.
- [10] P.C. Brooks, R.A. Clark, D.A. Chersesh, Requirement of vascular integrin alpha v beta 3 for angiogenesis, *Science* 264 (1994) 569–571.
- [11] W. Arap, R. Pasqualini, E. Ruoslahti, Cancer treatment by targeted drug delivery to tumor vasculature in a mouse model, *Science* 279 (1998) 377–380.
- [12] E.A. Murphy, B.K. Majeti, L.A. Barnes, M. Makale, S. Weis, K. Lutu-Fuga, W. Wrasidlo, D. Chersesh, Nanoparticle-mediated drug delivery to tumor vasculature suppresses metastasis, *Proc. Natl. Acad. Sci. U. S. A.* 105 (2008) 9343–9348.
- [13] E. Garanger, D. Botutyn, J.L. Coll, M. Favrot, P. Dumy, Multivalent RGD synthetic peptide as potent alpha v beta 3 integrin ligands, *Org. Biomol. Chem.* 4 (2006) 1958–1965.
- [14] B. Cacciari, G. Spalluto, Non peptidic alphaV-beta3 antagonists: recent developments, *Curr. Med. Chem.* 12 (2005) 51–70.
- [15] A. Meyer, J. Auernheimer, A. Modlinger, H. Kessler, Targeting RGD recognizing integrins: drug development, biomaterial research, tumor imaging and targeting, *Curr. Pharm. Des.* 12 (2006) 2723–2747.
- [16] U. Hersel, C. Dahmen, H. Kessler, RGD modified polymers: biomaterials for stimulated cell adhesion and beyond, *Biomaterials* 24 (2003) 4385–4415.
- [17] K. Temming, R.M. Schiffelers, G. Molema, R.J. Kok, RGD-based strategies for selective delivery of therapeutics and imaging agents to the tumor vasculature, *Drug Resist. Updates* 8 (2005) 381–402.
- [18] A.K. Singla, A. Garg, D. Aggarwal, Paclitaxel and its formulations, *Int. J. Pharm.* 235 (2002) 179–192.
- [19] P.B. Schiff, J. Fant, S.B. Horwitz, Promotion of microtubule assembly *in vitro* by taxol, *Nature* 277 (1979) 665–667.
- [20] R.B. Weiss, R.C. Donehower, P.H. Wiernik, T. Ohnuma, R. Gralla, D. Trump, J. Baker, D. Van Echo, D. Von Hoff, B. Leyland-Jones, Hypersensitivity reactions from taxol, *J. Clin. Oncol.* 8 (1990) 1263–1268.
- [21] F. Danhier, N. Lecouturier, B. Vroman, C. Jérôme, J. Marchand-Brynaert, O. Feron, V. Préat, Paclitaxel-loaded PEGylated PLGA-based nanoparticles: *in vitro* and *in vivo* evaluation, *J. Control. Release* 133 (2009) 11–17.
- [22] M. Garinot, V. Fievez, V. Pourcelle, F. Stoffelbach, A. des Rieux, L. Plapied, I. Theale, H. Freichels, C. Jerome, J. Marchand-Brynaert, Y.J. Schneider, V. Préat, PEGylated PLGA-based nanoparticles targeting M cells for oral vaccination, *J. Control. Release* 120 (2007) 195–204.
- [23] V. Pourcelle, S. Devouge, M. Garinot, V. Préat, J. Marchand-Brynaert, PCL-PEG-based nanoparticles grafted with GRGDS peptide: preparation and surface analysis by XPS, *Biomacromolecules* 8 (2007) 3977–3983.
- [24] V. Fievez, L. Plapied, A. des Rieux, V. Pourcelle, H. Freichels, V. Wascotte, M.L. Vanderhaeghen, C. Jérôme, A. Vanderplasschen, J. Marchand-Brynaert, Y.J. Schneider, V. Préat, Targeting nanoparticles to M cells with non-peptidic ligands for oral vaccination, *Eur. J. Pharm. Biopharm.* 73 (2009) 16–24.
- [25] L.W. Cao, H. Wang, J.S. Li, H.S. Zhang, 6-Oxy-(*N*-succinimidyl acetate)-9-(2-methoxycarbonyl) fluorescein as a new fluorescent labeling reagent for aliphatic amines in environmental and food samples using high-performance liquid chromatography, *J. Chromatogr. A* 1063 (2005) 143–151.
- [26] M.L. Zweers, G.H. Engbers, D.W. Grijpma, J. Feijen, *In vitro* degradation of nanoparticles prepared from polymers based on DL-lactide, glycolide and poly(ethylene oxide), *J. Control. Release* 100 (2004) 347–356.
- [27] V. Pourcelle, H. Freichels, F. Stoffelbach, R. Auzély-Velty, C. Jérôme, J. Marchand-Brynaert, Light induced functionalization of PCL-PEG block copolymers for the covalent immobilization of biomolecules, *Biomacromolecules* 10 (2009) 966–974.
- [28] D. Heckmann, A. Meyer, L. Burkhardt, G. Zahn, R. Stragies, H. Kessler, Rational design of highly active and selective ligands for the alpha5-beta1 integrin receptor, *Chem. Biol. Chem.* 9 (2008) 1397–1407.
- [29] S. Biltresse, M. Attolini, G. Dive, A. Cordi, G.C. Tucker, J. Marchand-Brynaert, Novel RGD-like molecules based on the tyrosine template: design, synthesis and biological evaluation on isolated integrins alphaV-beta3/alphaIIb-beta3 and in cellular adhesion tests, *Bioorg. Med. Chem.* 12 (2004) 5379–5393.
- [30] S. Biltresse, M. Attolini, J. Marchand-Brynaert, Cell adhesive PET membranes by surface grafting of RGD peptidomimetics, *Biomaterials* 26 (2005) 4576–4587.
- [31] X. Xiong, Y. Huang, W. Lu, X. Zhang, H. Zhang, T. Nagai, Q. Zhang, Enhanced intracellular delivery and improved antitumor efficacy of doxorubicin by sterically stabilized liposomes modified with a synthetic RGD mimetic, *J. Control. Release* 107 (2005) 262–275.
- [32] R.A. Swerlick, K.H. Lee, L.J. Li, N.T. Sepp, S.W. Caughman, T.J. Lawley, Regulation of vascular cell adhesion molecule 1 on human dermal microvascular endothelial cells, *J. Immunol.* 149 (1992) 698–705.
- [33] A.W. Griffioen, C.A. Damen, G.H. Blijham, G. Groenewegen, Tumor angiogenesis is accompanied by a decreased inflammatory response of tumor-associated endothelium, *Blood* 88 (1996) 667–673.
- [34] C. Lohbach, D. Neumann, C.M. Lehr, A. Lamprecht, Human vascular endothelial cells in primary cell culture for the evaluation of nanoparticle bioadhesion, *J. Nanosci. Nanotechnol.* 6 (2006) 3303–3309.
- [35] B. Jordan, P. Sonveaux, O. Feron, V. Gregoire, N. Beghein, B. Gallez, Nitric oxide-mediated increase in tumor blood flow and oxygenation of tumors implanted in muscles stimulated by electric pulses, *Int. J. Radiat. Oncol. Biol. Phys.* 55 (2003) 1066–1073.
- [36] P.S. Muether, S. Dell, N. Kociok, G. Zahn, D. Vossmeier, A. Jousen, The role of integrin alpha 5 beta 1 in the regulation of corneal neovascularization, *Exp. Eye Res.* 85 (2007) 356–365.
- [37] C. Jérôme, P. Lecomte, Recent advances in the synthesis of aliphatic polyesters by ring-opening polymerization, *Adv. Drug Deliv. Rev.* 60 (2008) 1056–1076.
- [38] A. des Rieux, V. Fievez, M. Momtaz, C. Detrembleur, M. Alonso-Sande, J. Van Gelder, A. Cauvin, Y.J. Schneider, V. Préat, Helodermin-loaded nanoparticles: characterization and transport across an *in vitro* model of the follicle-associated epithelium, *J. Control. Release* 118 (2007) 294–302.
- [39] C. Fonseca, S. Simoes, R. Gaspar, Paclitaxel-loaded PLGA nanoparticles: preparation, physicochemical characterization and *in vitro* anti-tumoral activity, *J. Control. Release* 83 (2002) 273–286.
- [40] A.J. Schraa, R.J. Kok, A.D. Berendsen, H. Moorlag, E. Bos, D. Meijer, L. de Leij, G. Molema, Endothelial cells internalize and degrade RGD-modified proteins developed for tumor vasculature targeting, *J. Control. Release* 83 (2002) 241–251.
- [41] H. Hall, V. Djonov, M. Ehrbar, M. Hoehli, J.A. Hubbell, Heterophilic interactions between cell adhesion molecule L1 and alphavbeta3-integrin induce HUVEC process extension *in vitro* and angiogenesis *in vivo*, *Angiogenesis* 7 (2004) 213–223.
- [42] H. Yoo, K. Lee, J. Oh, T. Park, *In vitro* and *in vivo* anti-tumor activity of nanoparticles based on doxorubicin-PLGA conjugates, *J. Control. Release* 68 (2000) 419–431.
- [43] Z. Hu, F. Luo, Y. Pan, C. Hou, L. Ren, J. Chen, J. Wang, Y. Zhang, Arg-Gly-Asp (RGD) peptide conjugated poly(lactic acid)-poly(ethylene oxide) micelle for targeted drug delivery, *J. Biomed. Mater. Res. A* 85 (2008) 797–807.
- [44] J.H. Park, S. Kwon, J.O. Nam, R. Park, H. Chung, S. Seo, I. Kim, I. Kwon, J. Jeong, Self-assembled nanoparticles based on glycol chitosan bearing 5 beta-cholanic acid for RGD peptide delivery, *J. Control. Release* 95 (2004) 579–588.
- [45] J.O. Nam, J.E. Kim, H.W. Jeong, Identification of the alpha v beta 3 integrin-interacting motif of beta1g-h3 and its anti-angiogenic effect, *J. Biol. Chem.* 278 (2003) 25902–25909.
- [46] M. Roberts, S. Barry, A. Woods, P. van der Sluijs, J. Norman, PDGF-regulated rab-4 dependent recycling of alpha v beta 3 integrin from early endosomes is necessary for cell adhesion and spearing, *Curr. Biol.* 11 (2001) 1392–1402.
- [47] M. Breunig, S. Bauer, A. Goepferich, Polymers and nanoparticles: intelligent tools for intracellular targeting? *Eur. J. Pharm. Biopharm.* 68 (2008) 112–128.
- [48] A. des Rieux, V. Fievez, M. Garinot, Y.J. Schneider, V. Préat, Nanoparticles as potential oral delivery systems of proteins and vaccines: a mechanistic approach, *J. Control. Release* 116 (2006) 1–27.